Exceptionally Long-Range Self-Assembly of Hexa-*peri*-hexabenzocoronene with Dove-Tailed Alkyl Substituents

Wojciech Pisula, Marcel Kastler, Daniel Wasserfallen, Tadeusz Pakula, and Klaus Müllen*

Max-Planck Institut für Polymerforschung, 55128 Mainz, Germany

Received March 23, 2004; E-mail: muellen@mpip-mainz.mpg.de

Electronic devices based on organic semiconductors have gained increased attention in nanotechnology, especially applicable to the field of field-effect transistors[1] and photovoltaics.[2] A promising class of materials in this research field is discotic liquid crystals. The disclike molecules arrange into one-dimensional columnar super-structures due to strong interactions between the aromatic cores. Hexa-*peri*-hexabenzocoronenes (HBC) exhibit some of the highest values for the intrinsic charge carrier mobility for mesogens, which makes them promising candidates for electronic devices.[3] Prereq-uisites for efficient charge carrier transport between electrodes are a high purity of the material to reduce possible trapping sites for charge carriers and a pronounced and defect-free,[4] long-range order.[5]

Appropriate processing techniques are required to induce a high degree of aligned structures in the discotic material. Highly ordered surface layers of different discotics, in particular of HBC derivatives, have been previously obtained by using Langmuir−Blodgett-,[6] zone-casting techniques,[7] or solution casting onto preoriented PTFE substrates.[8] The long-range order achieved by the latter protocol proved to be suitable for field effect transistors (FET).[8a]

Herein, a new HBC derivative with six branched, space-demanding, alkyl side chains is presented. The key feature of the implemented chain is the close proximity of the branching site to the aromatic core, which dramatically influences the self-organiza-tion behavior. This system perfectly fulfils the described de-mands: extraordinary long-range self-ordering, high purity, and facile processing from the isotropic state due to its low isotropization temperature.

Scheme 1 shows the previously described,[9] straightforward synthetic route for C6-symmetric HBC derivatives. The alkylbro-mide **3**, obtained from the commercially available alcohol **2**, was converted into the Grignard reagent which was subsequently coupled in a Kumada-type reaction with 4,4′-dibromodipheny-lacetylene.[10] The alkylated diphenylacetylene **5** was cyclotrimerized to the hexaphenylbenzene derivative **6**, and planarized with iron-(III)chloride in the final step to yield the HBC-C$_{14,10}$ **1** on a multigram scale.

Unlike other HBCs,[9a] it was possible to purify the substance by normal preparative column chromatography with hexane as the eluent. Inorganic and organic impurities were efficiently removed, so that the desired compound **1** was obtained at high purity.[11] Moreover, **1** is the first HBC known to be soluble in nonpolar solvents, such as pentane or hexane.

The thermal behavior of **1** as monitored by differential scanning calorimetry (DSC) revealed a phase transition from a "waxy-soft" crystalline phase to the isotropic melt at 46 °C. Compared to other *n*-alkyl-substituted HBCs, the isotropization temperature was shifted considerably from approximately 420 °C (above decomposition) to 46 °C.[9] To obtain information about the supramolecular organization of the compound, the phases were investigated using polarized optical microscopy (POM). Surprisingly, well-ordered spherulites nucleated randomly over the whole sample during the

Scheme 1[a]
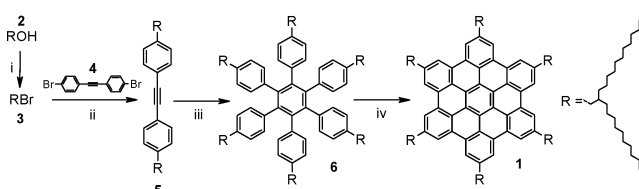
[a] Synthesis of HBC-C$_{14,10}$ **1**: i) NBS, PPh$_3$, CH$_2$Cl$_2$, 0 °C; ii) Mg, Cl$_2$Pd[dppf] x CH$_2$Cl$_2$, THF; iii) Co$_2$(CO)$_8$, dioxane, reflux, 24 h; iv) FeCl$_3$, CH$_3$NO$_2$, CH$_2$Cl$_2$, 25 °C, 45 min.
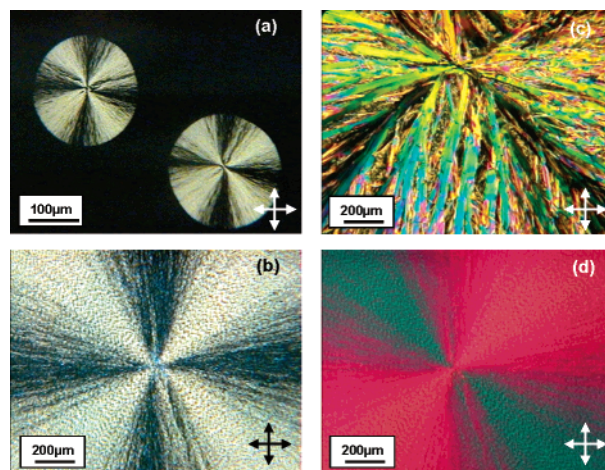

Figure 1. Cross-polarized optical microscopy images of HBC-C$_{14,10}$ **1** (a) during isothermal crystallization at 35 °C; (b) crystallized at 38 °C; (c) crystallized at 45 °C; (d) POM image from (c) using a λ-plate. All samples were crystallized between two glass slides.

cooling procedure (Figure 1a). This crystallization behavior is atypical for discotic systems, and spherulite formation of discotics has been published only for low-molecular mass liquid crystals[12] or discotics with substantially smaller cores.[13]

The spherulites revealed high anisotropy and therefore coherent long-range order. This was expressed by the Maltese cross,[12] where the isogyres followed the extinction of the analyzer/polarizer direction, indicating a radial alignment of columns from the center. Consequently, the columns were oriented in the spherulite growth direction with an edge-on arrangement of the molecules. Using a λ-plate and analyzing the yellow-blue distributions in the optical spherulite image, it was possible to determine that the spherulites are optically negative; i.e., the refractive index parallel to the radial direction is smaller than that perpendicular to it (Figure 1d). The observed textures proved a spontaneous self-assembly of **1** over several hundreds of micrometers. Upon closer inspection of different spherulites, a macroscopic periodicity along the radius was discovered. The periodic contrast, due to birefringent effects, appears on single fibrous structures, suggesting a helical twist of crystallites within the fibers,[14] as presented in Figure 2. Extinction
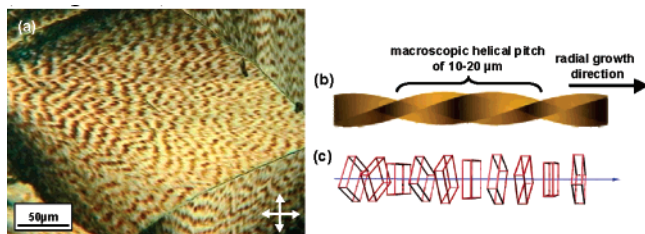
Figure 2. (a) Example of a cross-polarized optical microscopy image illustrating the periodic features along the spherulite radius, (b) schematic illustration of the helical fibrous structure, and (c) schematic presentation of the twist of the crystallites within the fibers.
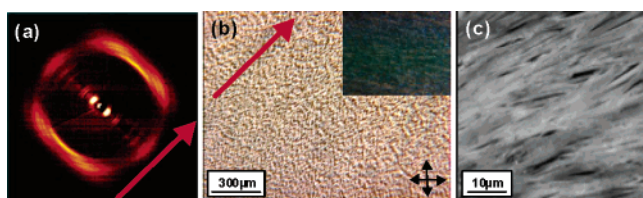

Figure 3. (a) 2D-WAXS of the zone-crystallized sample; the arrow indicates the moving direction of the sample; (b) POM image of the same sample positioned 45° from the polarizer/analyzer axes (inset: same image at 0° from the polarizer/analyzer axes); (c) AFM topography of zone-crystallized **1** revealing long fibrous structures.

occurred when the optical axis of crystallites coincided with the polarization plane (see Figure 2a,b).

The investigation of the crystallization kinetics revealed that the size of the spherulites was not significantly temperature dependent up to 35 °C. Above this temperature, the size increased exponentially, even exceeding 4 mm when crystallized isothermally at 40 °C. At temperatures higher than 44 °C, the texture changed, exposing a more colorful image (Figure 1b). Both the absence of the Maltese cross and the lower contrast of the textures reflected the absence of long-range order.

The remarkable self-assembly behavior of **1**, consisting of nucleation and directed structural growth, suggested the use of zone-crystallization technique[15] to obtain macroscopically controlled order for possible application in electronic devices. Indeed, after zone-crystallization, the sample revealed a high, homogeneous structural order with columns oriented uniaxially, edge-on (along the temperature gradient), as could be seen in the 2D-WAXS pattern (Figure 3a). Furthermore, the pattern indicated an intracolumnar distance of 0.48 nm and the molecules were tilted with respect to the columnar axis. The observed high optical anisotropy of the POM images confirmed the long-range order over large areas (Figure 3b). The topography of the zone-crystallized film imaged using AFM displayed fibrous morphology (Figure 3c). These structures were at least 100 μm long, 1–2 μm wide, and aligned in the moving direction of the sample during the processing; the strands were threaded and intertwined.

The introduction of a space-filling side chain is necessary to efficiently reduce aggregation.[16] In addition, it enables a better preparative purification. The use of the 2-decyltetradecyl chain fulfills the essential needs for the device fabrication: the branching at the β-position combined with the rotational freedom around the HBC-C$_\alpha$ bond induces a large steric demand and decreases the strong interaction of the aromatic core. As a result, the isotropization temperature was significantly reduced along with a much higher solubility. These two attributes are very desirable for simplifying

the processing of organic materials. Because of the decreased interaction, the self-assembly into superstructures is modulated and therefore leads to low nucleation rates and a formation of larger, ordered spherulites. The long, flexible, hydrophobic alkyl chains force the system to minimize contact with polar substrates such as glass or ITO, which results in an edge-on alignment of the molecules.

In conclusion, the first discotic system with an exceptional self-organization behavior over long-range to form spherulite textures was reported. This system is a promising candidate as an active component of electronic devices, due to its great processability and modulated, self-organization behavior.

Supporting Information Available: Experimental procedures and characterization for **3**, **5**, and **6**; evaluation of the crystallization kinetics, zone-crystallization processing parameters, additional AFM data, and rheology results. This material is available free of charge via the Internet at http://pubs.acs.org.

References

(1) (a) Dimitrakopoulos, C. D.; Malenfant, P. R. L. *Adv. Mater.* **2002**, *14*, 99−116. (b) Horowitz, G. *Adv. Mater.* **1998**, *10*, 365−377.
(2) Brabec, C. J.; Sariciftci, N. S.; Hummelen, J. C. *Adv. Funct. Mater.* **2001**, *11*, 15−26.
(3) van de Craats, A. M.; Warman, J. M. *Adv. Mater.* **2001**, *13*, 130−133.
(4) Lemaur, V.; da Silva Filho, D. A.; Coropceanu, V.; Lehmann, M.; Geerts, Y.; Piris, J.; Debije, M. G.; van de Craats, A. M.; Senthilkumar, K.; Siebbeles, L. D. A.; Warman, J. M.; Brédas, J.-L.; Cornil, J. *J. Am. Chem. Soc.* **2004**, *126*, 3271−3279.
(5) (a) Adam, D.; Schuhmacher, P.; Simmerer, J.; Haussling, L.; Siemens-meyer, K.; Etzbach, K. H.; Ringsdorf, H.; Haarer, D. *Nature* **1994**, *371*, 141−143. (b) Boden, N.; Bushby, R. J.; Clements, J.; Movaghar, B.; Donovan, K. J.; Kreouzis, T. *Phys. Rev. B* **1995**, *52*, 13274−13280.
(6) (a) Karthaus, O.; Ringsdorf, H.; Tsukruk, V. V.; Wendorff, J. H. *Langmuir* **1992**, *8*, 2279−2283. (b) Reitzel, N.; Hassenkam, T.; Balashev, K.; Jensen, T. R.; Howes, P. B.; Kjaer, K.; Fechtenkötter, A.; Tchebotareva, N.; Ito, S.; Müllen, K.; Bjornholm, T. *Chem.-Eur. J.* **2001**, *7*, 4894−4901. (c) Mindyuk, O. Y.; Heiney, P. A. *Adv. Mater.* **1999**, *11*, 341−344.
(7) (a) Tracz, A.; Jeszka, J. K.; Watson, M. D.; Pisula, W.; Müllen, K.; Pakula, T. *J. Am. Chem. Soc.* **2003**, *125*, 1682−1683. (b) Piris, J.; Pisula, W.; Tracz, A.; Pakula, T.; Müllen, K.; Warman, J. *Liq. Cryst.* **2004**. In press.
(8) (a) van de Craats, A. M.; Stutzmann, N.; Bunk, O.; Nielsen, M. M.; Watson, M.; Müllen, K.; Chanzy, H. D.; Sirringhaus, H.; Friend, R. H. *Adv. Mater.* **2003**, *15*, 495−499. (b) Bunk, O.; Nielsen, M. M.; Solling, T. I.; van de Craats, A. M.; Stutzmann, N. *J. Am. Chem. Soc.* **2003**, *125*, 2252−2258. (c) Zimmerman, S.; Wendorff, J. H.; Weder, C. *Chem. Mater.* **2002**, *14*, 2218−2223.
(9) (a) Fechtenkötter, A.; Tchebotareva, N.; Watson, M.; Müllen, K. *Tetrahedron* **2001**, *57*, 3769−3783. (b) Herwig, P.; Kayser, C. W.; Müllen, K.; Spiess, H. W. *Adv. Mater.* **1996**, *8*, 510−513.
(10) Mio, M. J.; Kopel, L. C.; Braun, J. B.; Gadzikwa, T. L.; Hull, K. L.; Brisbois, R. G.; Markworth, C. J.; Grieco, P. A. *Org. Lett.* **2002**, *4*, 3199−3202.
(11) Confirmed by UV/vis spectroscopy, where the purified samples revealed a higher extinction coefficient.
(12) Hutter, J. L.; Bechhoefer, J. *J. Crystal Growth* **2000**, *217*, 332−343.
(13) Bushey, M. L.; Hwang, A.; Stephens, P. W.; Nuckolls, C. *J. Am. Chem. Soc.* **2001**, *123*, 8157−8158.
(14) Imai, H.; Oaki, Y. *Angew. Chem., Int. Ed.* **2004**, *43*, 1363−1368 and references therein.
(15) (a) Lovinger, A. J.; Gryte, C. C. *Macromolecules* **1976**, *9*, 247−253. (b) Liu, C. Y.; Bard, A. J. *Chem. Mater.* **2000**, *12*, 2353−2362.
(16) Concentration-dependent ^{1}H NMR studies were performed, showing the lower aggregation behavior in solution compared to other HBC derivatives.

JA048351R